Features of Formation of the Cyclone Wakes (Fluctuations in Seawater Temperature) in the Area of Cape Svobodny, the Southeastern Part of the Sakhalin Island

P. D. Kovalev [1, ✉], **V. A. Squire** [2], **D. P. Kovalev** [1], **A. I. Zaytsev** [3]

[1] *Institute of Marine Geology and Geophysics, Far East Branch of Russian Academy of Sciences, Yuzhno-Sakhalinsk, Russian Federation*
[2] *University of Otago, Dunedin, New Zealand*
[3] *Special Design Bureau of Marine Research Automation, Far East Branch of Russian Academy of Sciences, Yuzhno-Sakhalinsk, Russian Federation*
✉ *kovalev_pd@outlook.com*

Purpose. The purpose of this work is to study the particulars of the formation of cyclone wakes after the regular passage of cyclones over the area of the wave measurements, and to estimate the internal wave parameters along the track according to the field observations.
Methods and Results. The analysis of data from the field observations of sea waves and water temperature is presented. The measurements were carried out by a ARW-K14 device (autonomous recorder of the waves and water temperature) in the area of the Cape Svobodny on the southeastern coast of the Sakhalin Island at a depth about 8 m. The recorded time series of the sea level and temperature fluctuations, lasting about one and a half months, were subjected to spectral analysis using specialized *Kyma* spectral analysis software. Dominant temperature fluctuations reaching 8.5 °C with a 13.1 h period were detected in the upper mixed layer of the ocean. These fluctuations were identified as the cyclone wakes in the stage of their relaxation. Taking into account the synoptic circumstances that existed during the passage of several cyclones and the associated storms in the observation area, the authors investigated the presence or absence of a trace.
Conclusions. It is shown that if the next storm arrives earlier than 10 days after the previous one, the trace may be shorter or even absent due to active water mixing in the upper mixed layer of the ocean. For the data obtained, the value of the coefficient $\in$ in the expression $\omega = (1 + \in) f$, which connects the dominant frequency ω of internal waves, i.e. almost inertial oscillations in the trace of each typhoon, with the inertial frequency f (the Coriolis parameter determined by the geographical latitude of the water area where the waves propagate), is close to the value proposed in the paper by E. Kunze. Using a formula due to J. F. Price, the characteristic horizontal lengths of internal waves in the direction of movement inside the wakes of cyclones moving at a speed 15–35 knots are determined. These lengths range from 304.6 to 1066.1 km.

Keywords: cyclone, internal waves, cyclone wake, seawater temperature fluctuations, upper mixed layer

Acknowledgements: the Russian co-authors declare that this study was carried out in accordance with the state programs of the Institute of Marine Geology and Geophysics, and the Special Research Bureau of Automation of Marine Research of the Far Eastern Branch of Russian Academy of Sciences. They are also grateful to the staff of the Wave Dynamics and Coastal Currents Laboratory for collecting field data. Vernon A. Squire appreciates the continued support from the University of Otago over a long career to this day, and especially thanks the graduate students and students who have learned a lot along the way.

For citation: Kovalev, P.D., Squire, V.A., Kovalev, D.P. and Zaytsev, A.I., 2022. Features of Formation of the Cyclone Wakes (Fluctuations in Seawater Temperature) in the Area of Cape Svobodny, the Southeastern Part of the Sakhalin Island. *Physical Oceanography*, [e-journal] 29(1), pp. 30-46. doi: 10.22449/1573-160X-2022-1-30-46

DOI: 10.22449/1573-160X-2022-1-30-46

1. Introduction

The Laboratory of Wave Dynamics and Coastal Currents, Institute of Marine Geology and Geophysics, Far Eastern Branch of the Russian Academy of Sciences (hereinafter IMGG), has monitored oceanic phenomena in the coastal zones of Sakhalin Island and the Kuril Islands for many years, with the predominant purpose of clarifying the characteristics of the multifarious wave regimes that occur at specific locations in the vicinity. This goal notwithstanding, the data being reported in this paper were actually collected initially to allow benchmarking to be done between wave recorders equipped with different primary transducers but, because the instruments captured several powerful storms – including an especially strong one, the wave time series obtained were deemed to be of sufficient scientific interest that a supplementary analysis with a targeted oceanographic focus was warranted. Specifically, the authors were interested in quantifying marine processes associated with the inception and resilience of fluctuations that occur as a result of cyclones.

Several published articles informed the current study. For example, the work [1] examined the aquatic environment that arose during the passage of Hurricane Ivan, where currents exceeding 200 $cm \cdot s^{-1}$ were observed. Ivan entered the Caribbean Sea on 8 September, 2004 and then, travelling on a northwesterly trajectory, moved through the Yucatan Channel into the Gulf of Mexico on 14 September. It is noted that, during the relaxation stage which occurs after the passage of a hurricane, the most distinctive feature is often a three-dimensional wake of internal waves of near-inertial (NI) periods whose oscillations can last for several days. Waves of that kind have been recorded in the wakes of several other hurricanes [2–5].

It's believed [6–9] that NI oscillations are mainly generated in the surface mixed layer of the ocean by atmospheric disturbances such as storms, hurricanes and cyclones. Forceful winds supply kinetic energy to the upper mixed ocean layer, generating strong currents and NI internal waves that form after several Rossby tuning cycles [10, 11] and spread mainly into the deep ocean, reaching a depth of 1200 m a few days after hurricanes leave the region [12]. For instance, Alford et al. [13] found that 12–33% of these waves can reach a depth of 800 m at Papa station in the northeastern Pacific Ocean.

In point of fact, NI oscillations of internal waves with frequencies close to the local inertial frequency f have been observed in all ocean basins and in the entire ocean column [14–20]. However, most observations relate to episodic hurricanes rather than the mid-latitude cyclones that can often follow each other in rapid succession [21]. Destruction of NI waves can cause ocean mixing, which affects the dispersion of pollutants and the productivity of the sea [22–24], supports the thermohaline circulation of the ocean and modulates the climate [16].

Knowledge of the marine processes during the passage of hurricanes and storms is also very important when technical specifications are being formulated for the construction of marine platforms that can be affected by hurricanes [25]. In addition, accurate estimates of extreme conditions are essential for realistic modelling of oceanographic conditions and, consequently, for the development of correct design standards.

Whilst many authors [2, 26, 27] attest that quite a lot is known about the wake which hurricanes and typhoons leave behind in the upper layer of the water column when they pass over seas and oceans, detailed reliable measurements are still rare. This is because planning is hindered by the erratic predictability of the exact places of genesis and trajectories of these familiar influential atmospheric constituents.

Analysis of sea water temperature instabilities in the time series recorded by the current authors reveals the presence of wakes as well, with internal wave NI oscillations succeeding the passage of cyclones accompanied by storms at a coastal installation site located near Cape Svobodny at the eastern end of Mordvinova Bay on Sakhalin Island. On the other hand, long wakes with accompanying long fluctuations were not consistently observed after every storm.

In sum, therefore, and taking into account the comments made above, this article will investigate oscillations – including internal waves, during the passage of cyclones in the coastal zone of the eastern shoreline of Sakhalin Island, a region of both scientific and practical interest.

2. Observational data

2.1. *Temperature and sea level*

An autonomous ARW-14 wave meter with designated factory No. 2012 was installed in the neighbourhood of Cape Svobodny, Mordvinova Bay in the summer of 2020, to study features associated with wave propagation nearby. Both sea level and temperature were measured for a month and a half at a sampling interval of 1 s. Fig. 1 shows the location of device No. 2012 off Cape Svobodny in the inset, alongside a map of Sakhalin Island.

F i g. 1. Map of the region (*left*) and the locations of the wave and temperature meter ARW-K14 No. 2012 (*right*)

The observations resulted in a spectrogram of sea level fluctuations showing diurnal and semidiurnal tidal fluctuations in the level and including fluctuations in the level caused by several storms, one of which was recorded between 26–30 September, with a wave height of up to 3.6 m. The spectrogram of the current spectral density of sea level fluctuations was calculated for the range of periods from 2 s to 26 h (Fig. 2).

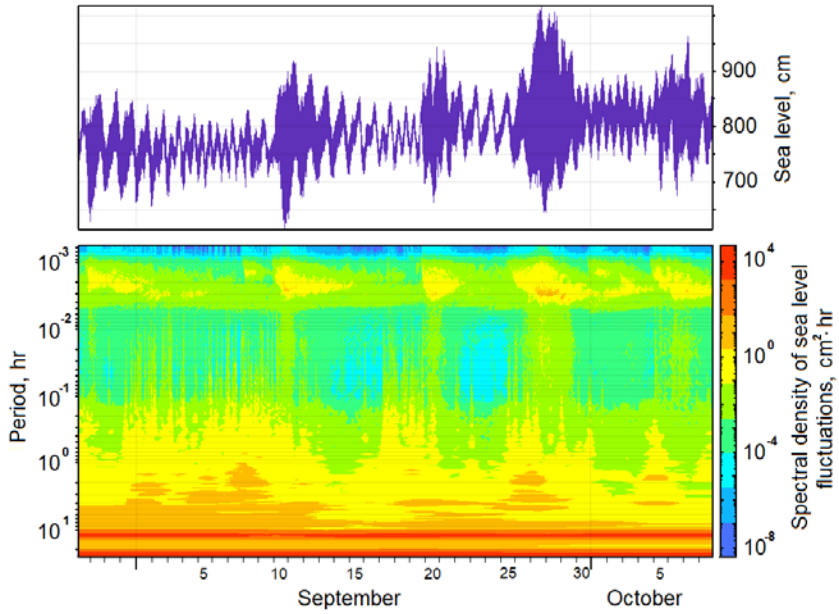

F i g. 2. Time series of sea level fluctuations and their spectrogram

Note that the visualization of the time series and the calculation of spectral densities were carried out using specialized software called *Kyma*, for complex processing and the analysis of time series of sea level and temperature fluctuations using proprietary algorithms based on the short-time Fourier transform [1]. The calculations employ the Kaiser – Bessel window technique of smoothing spectral estimates, and also take into account the coefficient of attenuation of surface waves with depth [28]. This software has been used repeatedly to calculate spectral densities in previously published articles. The parameters for calculating the spectral estimates used in the present paper were set based on the time series length or its segment to provide the required number of degrees of freedom and to identify the studied ranges of fluctuation periods, filtering background fluctuations in each specific case under consideration.

As the computed diagram of the current spectral density shows (Fig. 2), sea-level fluctuations at the observation point do not have any conspicuous features. Passing storms were accompanied by wind waves and only in the case of a strong storm did swell waves dominate. In the range of periods from 20 s to 8 min, which includes the infragravity wave band, a significant increase in energy is only observed during the strong storm from 26–30 September.

The spectrogram (Fig. 2) shows increasing oscillation energy in the band of periods from 1–12 h, which is not always associated with a storm situation. Additional spectral analysis of this range shows that the observed energy rise is not attributable to tidal fluctuations and does not have pronounced peaks. Nevertheless,

[1] Kovalev, P.D., 2018. *Kyma*. [computer program] Yuzhno-Sakhalinsk: Institute of Marine Geology and Geophysics, registration no. RU2018618773 (in Russian).

fluctuations with diurnal and semi-diurnal tidal waves are well distinguished near the bottom axis of the spectrogram.

Based on the measured fluctuations in water temperature, their changes were analyzed during the level observation period (Fig. 3). Sharp fluctuations in water temperature from about 7 to 12 °C are evident between 31 August and 9 September, with an average period of 13.1 h. A similar but shorter group of oscillations with a smaller amplitude is observed from 17–20 September. These groups appear after the storm has significantly weakened.

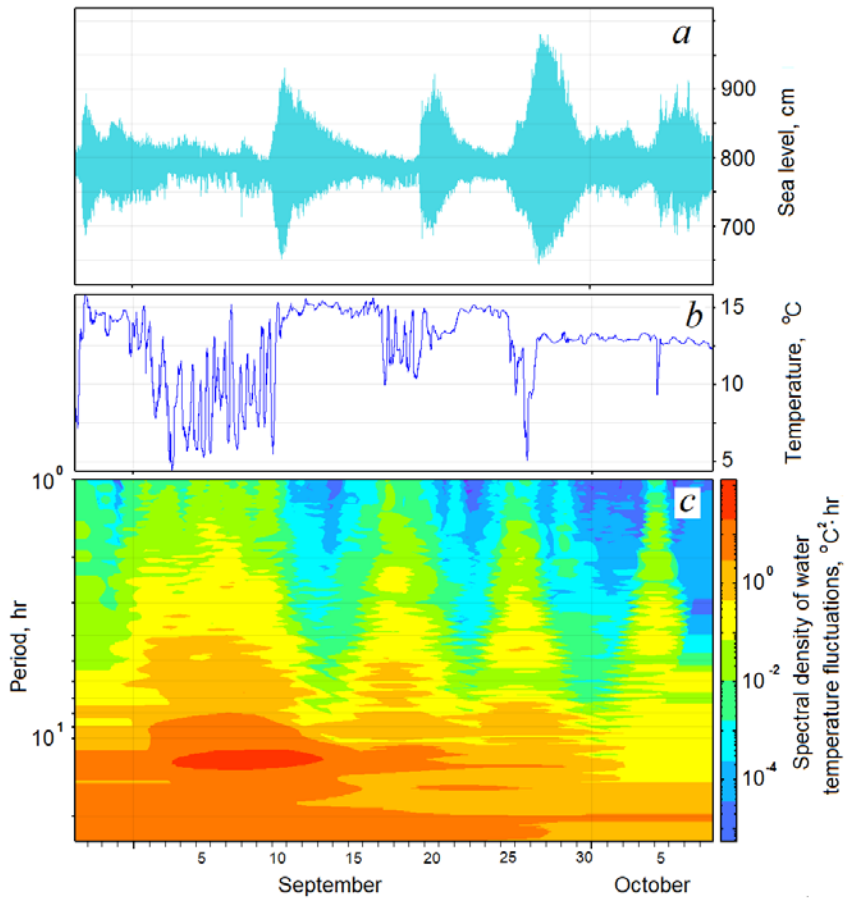

F i g. 3. Graphs of the sea level fluctuations with the subtracted pre-computed tide (*a*), seawater temperature (*b*), and diagram of the current spectral density of the water temperature fluctuations (*c*)

The spectrogram (Fig. 3, *c*) also shows a significant rise in the energy of oscillations with a period of about 13 h for the time of occurrence of these two groups of waves. The peak with a period of about 13 h is also clearly visible in the spectrum shown in Fig. 4, calculated from the temperature time series from 31 August to 10 September. Also note that the spectrum of these oscillations is broad and extends up to about 30 min, but the energy of temperature fluctuations drops sharply by four orders of magnitude compared to the main maximum.

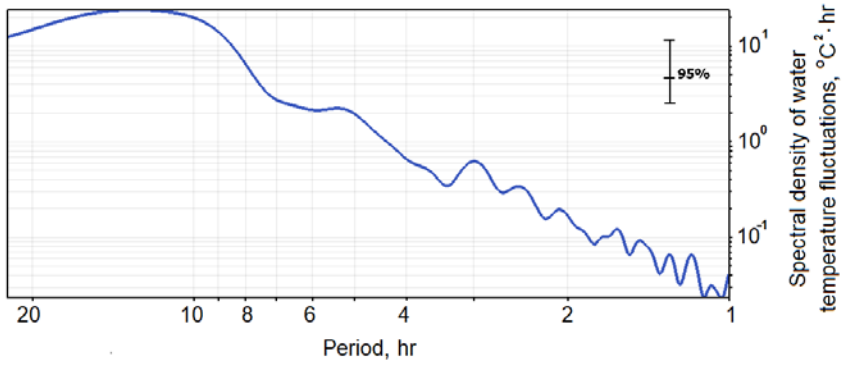

F i g. 4. The spectrum of temperature fluctuations calculated for the time series of temperature from 31 August to 10 September

The authors of the paper believe that the most distinctive feature of the relaxation stage is the three-dimensional trace of NI internal waves. Such waves have been observed in the tracks of several hurricanes (and in the cases considered here, cyclones), by various researchers, mainly in the Gulf of Mexico region [6–8]. In addition, the spectral analysis given in [4] demonstrated that the NI frequency is usually slightly higher than the local Coriolis parameter *f*.

In [1], NI motion is determined by a frequency between 0.9 *f* and 1.2 *f* [29]. At the same time, in [21] it is believed that the frequency of NI oscillations in the mixed layer is higher than the local inertial frequency by an amount approximately equal to half the Burger number of the mixed layer. In the case under consideration, for the latitude of Cape Svobodny (about 46.8°N), the period of NI movements according to Kunze is located between periods from 13.7 to 18.2 h. The period of 13.1 h obtained from our observations is evidently somewhat shorter, i.e. the frequency of detected internal cyclone wake waves is slightly higher.

Note that the NI frequency estimated from direct measurements given in [1], as in the case considered here, was approximately 4% and 9% higher than the Coriolis parameter *f* at the slope and outer shelf locations and approximately corresponded to the inertial frequency shift proposed and determined by the Burger number for the mixed layer [30].

2.2. *Synoptic evaluation*

It is of interest to analyze the reason why in some cases the wake of a cyclone is formed and expresses itself in variations in the temperature of seawater yet, in other cases, it does not. To do this, we will consider synoptic maps and trace the paths of typhoons that passed over Mordvinova Bay and Cape Svobodny during the observations of water temperature and waves. Figs. 5–8 show synoptic maps for situations where a sharp drop in temperature occurred,taken from the *Japan Meteorological Agency* open web-page [2].

[2] Japan Meteorological Agency. *Weather*. 2021. [online] Available at: www.jma.go.jp [Accessed 10 October 2021].

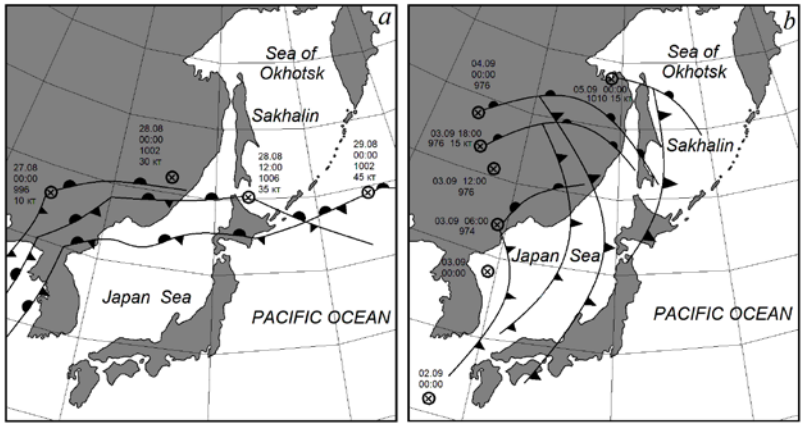

F i g. 5. Synoptic maps for the time periods August, 27 – September, 29 (*a*) and September, 2 – 5, 2020 (*b*)

Temperature fluctuations at a period of about 13 h began on 31 August, as shown by the temperature time series plotted in Figs. 3, *b*. It is clear that they were initiated by a cyclone moving rapidly at a speed of about 35 knots in an easterly direction and accompanied by a stationary front (Fig. 5, *a*). However, by 10 o'clock on 3 September, the impact of the cyclone had weakened significantly and the wave heights had reduced to just 40–60 cm. This decrease notwithstanding, it was on 3 September that the amplitudes of temperature fluctuations increased sharply and continued until the arrival of the next cyclone on 10 September.

A comparable increase in temperature was not observed in the wake of the cyclone that arrived on 10 September. The average amplitude of temperature fluctuations from 17 to 20 September was only about 1.7 °C, whilst after 3 September it was more than twice that. We also mention in passing that the observed temperature fluctuations which began on 31 August lasted about 10 d, which is consistent with the data of [1], whilst those that began on 17 September lasted only 3 d, although it is possible that their continuation was inhibited by the next cyclone.

To shed light on this phenomenon, the synoptic conditions in the observation area were analyzed, starting from 2 September. As the synoptic map shows (Fig. 5, *b*), after 2 September a cyclone moved in a northerly direction accompanied by warm and cold fronts. And, although the cyclone itself moved away from the area such that it was more than a 1000 km from the point of observation, its fronts passed over the southern part of Sakhalin Island and later over the entire island. It is possible that this was the reason for the prolonged large amplitude fluctuations in the temperature of the seawater. But more observations would be required to prove this conclusively.

The synoptic situation for the time period from 17–20 September, where the amplitudes of seawater temperature fluctuations were less than half as large as those observed after 3 September, is shown in Fig. 6. Fig. 6, *a* shows that from 9 to 10 September, a weak cyclone moved at a speed of about 15 knots over the southern part of Sakhalin Island, accompanied by stationary fronts. Taking into

account the observations being discussed here but also those of other authors, the 13-h-period trace of temperature took shape immediately following the cyclone and only lasted for about 5 d. This is roughly half of that for the first case considered, i.e. the usual temperature trace duration of 10 d [1].

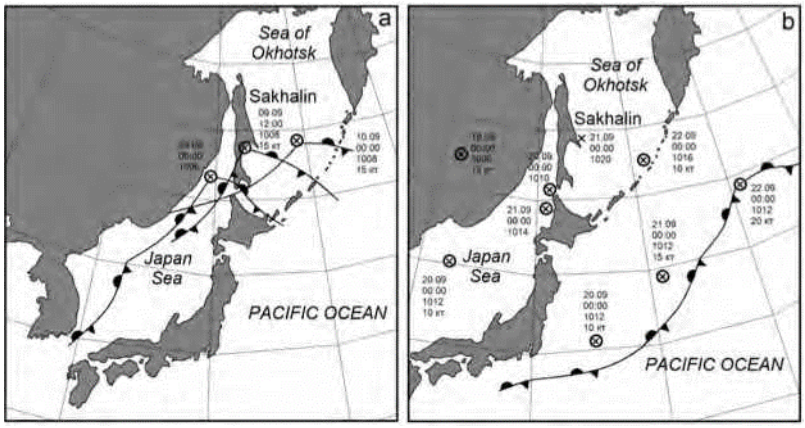

F i g. 6. Synoptic maps and pathways of cyclones 9–10 and 19–22 September 2020

Based upon the synoptic situation that developed after 10 September, it is concluded that the track of the cyclone – which asserted itself as a time series of temperature fluctuations, was destroyed on 20 September as a result of mixing of the upper quasi-homogeneous ocean layer. This was caused by the two cyclones that approached the region (Fig. 6, *b*), one of which moved from the continent and passed over the southern part of Sakhalin Island. No fronts were registered accompanying this cyclone. The second cyclone, also without associated fronts, approached from the south from the Sea of Japan and entered the Sea of Okhotsk a day later, on 21 September. These cyclones were attended by a storm in the area under consideration, which is clearly evident in Fig. 3, *a* by the increase in wave activity from the evening of 19 September.

At about 12:00 UTC on 18 September, a cyclone approached Sakhalin Island from the northwest, at a distance of about 150 km from the southernmost tip of the island; the cyclone subsequently changed direction and shifted to the northeast. This cyclone did not significantly increase wave activity in the area of Cape Svobodny, however, as can be seen from Fig. 3, *a*, which shows that the waves did not begin to grow until 19 September. An analysis of the synoptic maps shows that only weak winds with speeds of 0.5 to 3 $m \cdot s^{-1}$ were observed in the area of the southern tip of the island on 18 September and only a slight increase in the height of sea waves was observed in the vicinity of Cape Svobodny.

An interesting feature in the observed behaviour of the seawater temperature is identified immediately after the storm beginning on 9 September, clearly visible in Fig. 3, *b*. At the beginning of a decrease in storm waves for 3–4 d, fluctuations in the temperature of about 1.5 °C occur at the tidal period. A similar pattern is observed with the weakening of the waves after the storm of 19 September and a weak storm that began on 5 October.

The 19-September storm, composed of two cyclones as noted, arrived at the observation point around 21:00 UTC (Fig. 6, *b*). In the beginning, a situation similar to the first cyclone considered developed, i.e. a sharp drop in water temperature occurred on 25–26 September (Fig. 3, *b*) resembling the formation of a typhoon wake. At the same time, a zone of high pressure was located over the northern part of the Sea of Okhotsk from 23–27 September (Fig. 7), which contributed to a decrease in wave height and the beginning of the relaxation stage after the cyclone.

However, on 25 September, a new storm approached the observation area from the south and the height of the waves began to increase. Then wave growth eased before building again at around 17 h on 26 September. Contemporaneously, the speed of the east wind at the southern tip of Sakhalin reached up to 14 to 16 $m \cdot s^{-1}$. Most likely, this storm led to mixing of the water column and the destruction of the wake that had started to form.

On the graph of seawater temperature fluctuations (Fig. 3, *b*), there is another significant drop in temperature of about 3.5 °C, observed on 5 October 2020 but only lasting about 5 h. The reason for this decrease in temperature could be two cyclones, the first of which (Fig. 7) caused a storm in the observation area that began on 25 September. The second, weaker cyclone with a pressure at its centre of 1010 mbar, gradually deepened as it moved over the coastline of Primorsky Krai on 2–3 October. The synoptic situation for this case is shown in Fig. 8, *a*. A small increase in wave height due to the cyclone – exceeding the background level, was registered at the observation point and is visible on 3 October in Fig. 3, *a*.

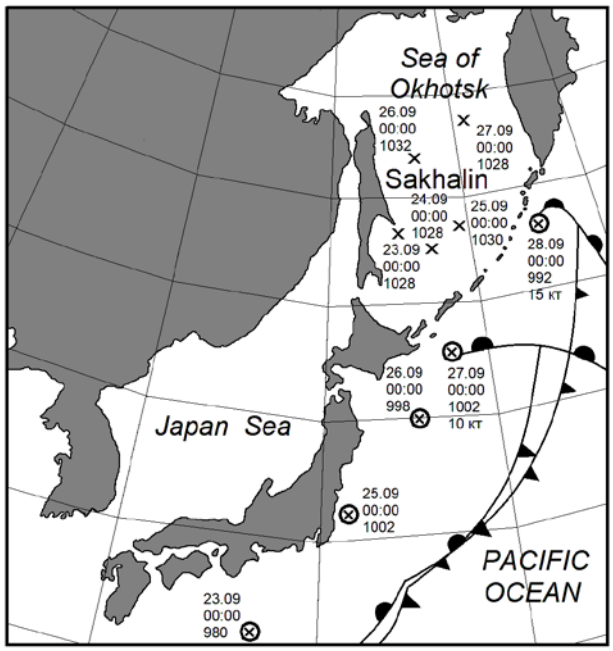

F i g. 7. Synoptic maps for September, 23–28, 2020

It is difficult to determine reliably which of the cyclones caused the temperature drop on 5 October when the cyclone's wake appears to start to form. The authors are inclined to believe that the feature is due to the cyclone that carried the 25-September storm since the time necessary for relaxation of the sea after this cyclone passed is several days, as noted earlier. During the storm on 3 October, the height of the waves was a factor three smaller, so enough relaxation would occur only a day before the sharp drop in the temperature of the upper mixed layer of the sea.

By 5 October a baric system consisting of two cyclones approached the southern part of Sakhalin Island (Fig. 8, *b*) moving in an easterly direction. By about 3:00 UTC on 5 October, the centre of the first cyclone was located over the southern tip of the island. It was followed at a distance of 400–500 km by a second cyclone, the centre of which at 18 h on 5 October was also over Aniva Bay at the far south of Sakhalin Island, whilst the centre of the first cyclone shifted to a latitude of 50°N roughly half way up the island. Simultaneously, Fig. 3, *b* suggests that strong mixing of the sea's upper mixed layer was continuing, as the temperature did not increase but remained at about 13 °C which violated the conditions for further formation of the cyclone's wake.

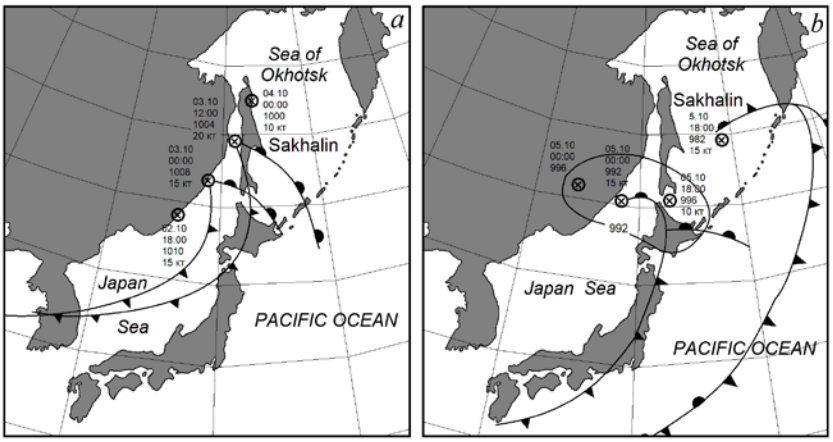

F i g. 8. Synoptic maps for October, 2–4 (*a*) and October, 5 (*b*), 2020

Based on the above discussion, namely on the behaviour of seawater temperature and synoptic conditions, the authors have reached the conclusion that the start of anomalous traces in the various data series – and hence each relaxation stage, is only weakly related to the wave height. This is because in the first case considered, the wave height in the storm that began on 28 September was about 1.75 m, at which fluctuations in the wake temperature were formed and reached 8.5 °C. When the storm began on 10 September, the height of the waves reached 2.75 m but the temperature fluctuations were only about 4 °C. At the same time, the time interval from the beginning of the storm to the appearance of temperature fluctuations in the wake varies from 3 d for the first case to 6 d in the second case. Apparently, the time before the beginning of the relaxation stage depends on

the duration of the storm and, as a result, the coverage of a larger water area, which, after agitation, will fade more slowly.

3. Internal wave generation

Many authors [1, 31, 32], agree that most of the internal wave motion in the ocean occurs as a result of the wind and other surface influences. The authors of [33, 34] amongst other oceanographers, also conclude that because the velocity of atmospheric fronts is usually much greater than the phase velocity of internal waves in the ocean, the ocean reacts in two stages: a first, short stage, when currents arise in the ocean's surface layer; and a second, longer stage, when waves after the cessation of exposure undergo geostrophic adjustment (the Rossby adjustment) [31].

Note that geostrophic adjustment is a process in geophysical hydrodynamics, when the fields of the initial perturbation of pressure and velocity in a rotating fluid are mutually deformed until a stationary balance is established between the pressure gradient and the Coriolis force belonging to the stationary velocity field. This final state is called geostrophic equilibrium. This problem was first theoretically solved by Carl-Gustaf Rossby and for this reason is called the "Rossby adjustment". On rotating planets with an atmosphere, as well as those with oceans in which the corresponding Rossby radii are smaller than the radius of the corresponding planet, geostrophic adaptation is a fundamental process that largely determines the dynamics of their atmospheres and oceans [3].

When waves of NI frequency are generated with the difference between their angular frequency ω and the local inertial frequency f depending on the horizontal wave number (k, l) for the disturbance left by the storm. This is determined by the equation [31]

$$\omega^2 - f^2 = c_j^2 \kappa^2 = c_j^2(k^2 + l^2),$$

where c_j is an eigenvalue that is physically the phase speed associated with the jth vertical baroclinic internal mode, (k, l) – is the two-dimensional wave number.

Garrett [31] proposes that the NI range should extend from f to $(1 + \in) f$, and that the value of $\in$ can take a value up to 1 on the basis that the Coriolis force and the buoyancy force are equally important at a frequency of $2f$. The quantity $\in$ is sometimes called the inertial shift [11]. If $\omega = (1 + \in) f$ and $\in$ is small enough that $\in^2$ can be neglected, then Eq. (1) gives

$$\in = \in_j \approx \frac{1}{2} (c_j/f)^2 \kappa^2 , \qquad (1)$$

where $R_j = c_j / | f |$ is the associated Rossby j-radius. Garrett suggests a typical value for mid-latitudes is 30 km for the first mode and less for higher modes, giving $\in \approx 0.05$ for the first mode if $\kappa^{-1} \approx 100$ km, which decreases with the mode number [31].

The authors decided to investigate possible values of $\in$ for the observations reported in the current paper. Two methods for determining the value of $\in$ are

[3] Wikimedia Foundation Inc. *Geostrophische Anpassung*. 2022. [online] Available at: https://de.wikipedia.org/wiki/Geostrophische_ Anpassung [Accessed: 11 January 2022].

considered to find out the one that will give a comparable result with previously published results. When analyzing the scientific literature on the subject under consideration, the authors came across at least two methods, and here, as can be seen below, they give similar results. Therefore, it would be wrong not to consider both methods and not to compare the results. In addition, the analysis of the existing oceanographic literature did not show the advantages of either method, which would allow it to be preferred.

Method I utilizes R, at the installation location of the instrument. In [35] it is reported that the Brunt-Vaisala frequency N off Sakhalin Island in July lies from 0.01 s^{-1} to 0.038 s^{-1} and is centred on 0.025 s^{-1}. Regarding N as a depth-averaged quantity and using R, = $NH/\ jnf$ [36, 37], where H = 50 m is the depth and $f = 1.06 \cdot 10^{-4}$ s^{-1}, indicates the Rossby radius for j = 1 will lie in the range 1.50–5.70 km, centred around 3.75 km. These values are comparable to those documented in [38] on the Sakhalin Island shelf.

Formula (1) can be used to find $\in$, in principle, recognizing that a value for K is required and that the value used in [31] for 30°N is likely to be too small for NI wave numbers at the higher latitude of 46.8°N on the Sakhalin Island shelf in the Sea of Okhotsk. Accordingly, an estimate wavelength of 40 km is used [39, 40]. With this value, Eq. (1) gives $0.028 < \in < 0.40$ centred around $\in = 0.17$. The reader is reminded, however, that the result of this calculation is strongly dependent on the horizontal wavelength chosen. It is noted that, whilst the range of values specified for $\in$ includes those found by other authors [11, 30], it extends to slightly higher values that will reflect the nature of the coastal oceanography of the Sea of Okhotsk.

Method II uses the value of the frequency (period) of the internal waves observed during the experiment that is being reported herein and the formula $\omega = (1 + \in) f$, suggested by Garrett (2001) and Price (1983), who used v rather than e). The Coriolis frequency in the vicinity of our observations at Cape Svobodny is $f = 1.06 \cdot 10^{-4}$ s^{-1} (inertial period 16.4 h), whilst the NI frequency ω was measured as $\omega = 2.12 \cdot 10^{-5}$ s^{-1} = $1.33 \cdot 10^{-4}$ $rads^{-1}$ (period 13.1 h). Thus $\omega/f = 1.253$ and the small parameter $\in = 0.253$, which is within the range found by Method I. Contrariwise, if we take the central value of the Rossby radius, i.e. 3.75 km, we can find κ^2 and deduce that the horizontal wavelength of the internal waves is roughly 33 km.

A determinative characteristic of cyclones is the horizontal wavelength of the oscillatory movements of air in their wakes in the direction of propagation, which we denote by λ. This can be recovered from the equation obtained from the kinematic relation for the time-dependent wake $\frac{\partial}{\partial t} = U_H \frac{\partial}{\partial x}$, where $U_H \sim \omega\lambda/2\pi$ – is the velocity of the cyclone and, without loss of generality, the x-axis is now aligned with the direction of propagation of the wave. The wake resembles a surface-gravity wave following a steadily moving ship [21]. Then λ is given by

$$\lambda = \frac{2\pi}{\omega} U_{\mathrm{H}} = \frac{2\pi}{f(1+\in)} U_{\mathrm{H}} \approx \frac{2\pi}{f}(1-\in) U_{\mathrm{H}} \approx \frac{2\pi}{f} U_{\mathrm{H}} \ . \qquad (2)$$

The horizontal wavelengths for the observed velocities in the wakes of cyclones over Sakhalin Island are recorded in Table. Evidently, the velocities of every cyclone are much greater than the phase velocities of the spawned internal waves, which are typically about 2 m·s^{-1} [21] or less [41] – parenthetically, the phase speed of the first vertical baroclinic internal mode c_1 used in Method I varies between 0.16 and 0.60 m·s^{-1} for the values used. Therefore, according to the conclusions in [21], the baroclinic response to a storm includes a propagating trace of inertial-internal waves.

The speed of movement of cyclones and length of wake oscillations in the moving direction

Parameters	Dates of a storm start				
	28.08.2020	10.09.2020	19.09.2020	25.10.2020	2.10.2020–3.10.2020
Cyclone speed (knots)	35	15	15	10	15–20
Cyclone speed (m·s^{-1})	17.99	7.71	7.71	5.14	7.71–10.29
Wave length in the direction of movement	1066.1	456.9	456.9	304.6	456.9–609.8

Price [21] also gives a formula for the transverse horizontal wavelength, which is approximately $12R \approx 18$ km to 45 km for the cases considered here. The dimensions of the horizontal wavelengths in each cyclone's wake exceed the horizontal scales of the internal wave continuum by a goodly amount, suggesting that the initial horizontal proportions of the oscillatory trace in each cyclone's wake are directly influenced by the scales of the atmospheric determinants that expedite the oceanic outcomes observed. This is also the conclusion reached in [42].

Smaller horizontal scales and higher frequencies are generated by internal effects of finite amplitude when the atmospheric effect is intense, as recognized in [21] for the standard case. It is certainly possible that the peaks between 1 and 3.5 h that are evident in the energy density spectrum plotted in Fig. 4 exemplify these higher-frequency harmonics, although this assertion remains equivocal because their magnitudes are less than 95% of the confidence interval.

4. Conclusion

An analysis of seawater temperature fluctuations has been carried out — drawing also on sea surface elevation measurements, using a 42-day-long data set collected in the vicinity of Cape Svobodny on southeast Sakhalin Island using seafloor-mounted devices. Surface waves with heights in the range 1–3.6 m were present during the experiment's collection phase.

The records of seawater temperature fluctuations allowed the authors to detect four cases of significant (in comparison with the spread of background temperatures), periodic and non-periodic changes in temperature, reaching 8.5 °C with the background fluctuations only being about 1 °C. The average oscillation period was about 13.1 h. The oscillations themselves are attributed to internal waves that form in the so-called wake of the cyclone during relaxation after its passage.

It is established that the duration of the fluctuations present in the cyclone wake can reach 10 d, which is consistent with the data of other authors. An analysis of synoptic maps shows that in the case of the arrival of the next cyclone earlier than 10 d after the wake of the previous cyclone begins to form, a short wake is formed that is destroyed as a result of mixing in the upper layer of the ocean by storm waves. At the same time, two cases were observed when, after a sharp decrease in temperature and the arrival of a storm, the wake didn't form at all.

Based upon the behaviour of the seawater temperature and synoptic environment, it is shown that the beginning of wake formation and, consequently the relaxation stage, is only weakly related to the wave heights during the previous storm. The authors believe that the time before the beginning of the relaxation stage depends on the duration of the storm and, as a result, on the coverage of a larger water area, which, having been set in motion, will fade more slowly.

Using a formula originally due to Price it is shown that the coefficient $\in$ connecting the dominant frequency of internal waves, viz. NI oscillations, in the wake of a typhoon ω, with the inertial frequency f for the observed data is 0.253. This is close to the value of 0.2 proposed by Kunze. Using the Price's formula, the characteristic horizontal wavelengths of oscillations in the wake of several cyclones travelling at speeds of 15 to 35 knots in the direction of their movement span 304.6–1066.1 km.

REFERENCES

1. Teague, W.J., Jarosz, E., Wang, D.W. and Mitchell, D.A., 2007. Observed Oceanic Response over the Upper Continental Slope and Outer Shelf during Hurricane Ivan. *Journal of Physical Oceanography*, 37(9), pp. 2181-2206. https://doi.org/10.1175/JPO3115.1
2. Fedorov, K.N., Varfolomeev, A.A., Ginzburg, A.I., Zatsepin, A.G., Krasnopevtsev, A.Yu, Ostrovsky, A.G. and Sklyarov, V.E., 1979. Thermal Reaction of the Ocean on the Passage of the Hurricane "Ella". *Oceanology*, 19(6), pp. 992-1001 (in Russian).
3. Brooks, D.A., 1983. The Wake of Hurricane Allen in the Western Gulf of Mexico. *Journal of Physical Oceanography*, 13(1), pp. 117-129. https://doi.org/10.1175/1520-0485(1983)013<0117:TWOHAI>2.0.CO;2
4. Shay, L.K. and Elsberry, R.L., 1987. Near-Inertial Ocean Current Response to Hurricane Frederic. *Journal of Physical Oceanography*, 17(8), pp. 1249-1269. https://doi.org/10.1175/1520-0485(1987)017<1249:NIOCRT>2.0.CO;2
5. Brink, K.H., 1989. Observations of the Response of Thermocline Currents to a Hurricane. *Journal of Physical Oceanography*, 19(7), pp. 1017-1022. https://doi.org/10.1175/1520-0485(1989)019<1017:OOTROT>2.0.CO;2
6. Leaman, K.D. and Sanford T.B., 1975. Vertical Energy Propagation of Inertial Waves: A Vector Spectral Analysis of Velocity Profiles. *Journal of Geophysical Research*, 80(15), pp. 1975-1978. https://doi.org/10.1029/JC080i015p01975

7. D'Asaro, E.A. and Perkins, H., 1984. A Near-Inertial Internal Wave Spectrum for the Sargasso Sea in Late Summer. *Journal of Physical Oceanography*, 14(3), pp. 489-505. https://doi.org/10.1175/1520-0485(1984)014<0489:ANIIWS>2.0.CO;2

8. Pinkel, R., 1984. Doppler Sonar Observations of Internal Waves: The Wavenumber-Frequency Spectrum. *Journal of Physical Oceanography*, 14(8), pp. 1249-1270. https://doi.org/10.1175/1520-0485(1984)014<1249:DSOOIW>2.0.CO;2

9. Sanford, T.B., 2013. Spatial Structure of Thermocline and Abyssal Internal Waves in the Sargasso Sea. *Deep Sea Research Part II: Topical Studies in Oceanography*, 85, pp. 195-209. https://doi.org/10.1016/j.dsr2.2012.07.021

10. Rossby, C.-G., 1938. On the Mutual Adjustment of Pressure and Velocity Distributions in Certain Simple Current Systems. *Journal of Marine Research*, 1(1), pp. 15-28. Available at: https://images.peabody.yale.edu/publications/jmr/jmr01-01-02.pdf [Accessed: 11 January 2022].

11. Qi, H., De Szoeke, R.A., Paulson, C.A. and Eriksen, C.C., 1995. The Structure of Near-Inertial Waves during Ocean Storms. *Journal of Physical Oceanography*, 25(11), pp. 2853-2871. https://doi.org/10.1175/1520-0485(1995)025<2853:TSONIW>2.0.CO;2

12. Morozov, E.G. and Velarde, M.G., 2008. Inertial Oscillations as Deep Ocean Response to Hurricanes. *Journal of Oceanography*, 64(4), pp. 495-509. https://doi.org/10.1007/s10872-008-0042-0

13. Alford, M.H., Cronin, M.F. and Klymak, J.M., 2012. Annual Cycle and Depth Penetration of Wind-Generated Near-Inertial Internal Waves at Ocean Station Papa in the Northeast Pacific. *Journal of Physical Oceanography*, 42(6), pp. 889-909. https://doi.org/10.1175/JPO-D-11-092.1

14. Pollard, R.T. and Millard Jr., R.C., 1970. Comparison between Observed and Simulated Wind-Generated Inertial Oscillations. *Deep Sea Research and Oceanographic Abstracts*, 17(4), pp. 813-821. https://doi.org/10.1016/0011-7471(70)90043-4

15. D'Asaro, E.A., 1985. The Energy Flux from the Wind to Near-Inertial Motions in the Surface Mixed Layer. *Journal of Physical Oceanography*, 15(8), pp. 1043-1059. https://doi.org/10.1175/1520-0485(1985)015<1043:TEFFTW>2.0.CO;2

16. Alford, M.H., 2003. Improved Global Maps and 54-year History of Wind-Work on Ocean Inertial Motions. *Geophysical Research Letters*, 30(8), 1424. doi:10.1029/2002GL016614

17. Guan, S., Zhao, W., Huthnance, J., Tian, J. and Wang, J., 2014. Observed Upper Ocean Response to Typhoon Megi (2010) in the Northern South China Sea. *Journal of Geophysical Research: Oceans*, 119(5), pp. 3134-3157. https://doi.org/10.1002/2013JC009661

18. Sanford, T.B., Price, J.F. and Girton, J.B., 2011. Upper-Ocean Response to Hurricane Frances (2004) Observed by Profiling EM-APEX Floats. *Journal of Physical Oceanography*, 41(6), pp. 1041-1056. https://doi.org/10.1175/2010JPO4313.1

19. Yang, B., Hou, Y., Hu, P., Liu, Z. and Liu, Y., 2015. Shallow Ocean Response to Tropical Cyclones Observed on the Continental Shelf of the Northwestern South China Sea. *Journal of Geophysical Research: Oceans*, 120(5), pp. 3817-3836. https://doi.org/10.1002/2015JC010783

20. Alford, M.H., MacKinnon, J.A., Simmons, H.L. and Nash, J.D., 2016. Near-Inertial Internal Gravity Waves in the Ocean. *Annual Review of Marine Science*, 8, pp. 95-123. https://doi.org/10.1146/annurev-marine-010814-015746

21. Price, J.F., 1983. Internal Wave Wake of a Moving Storm. Part I. Scales, Energy Budget and Observations. *Journal of Physical Oceanography*, 13(6), pp. 949-965. https://doi.org/10.1175/1520-0485(1983)013<0949:IWWOAM>2.0.CO;2

22. Price, J.F., 1981. Upper Ocean Response to a Hurricane. *Journal of Physical Oceanography*, 11(2), pp. 153-175. https://doi.org/10.1175/1520-0485(1981)011<0153:UORTAH>2.0.CO;2

23. Gregg, M.C., 1987. Diapycnal Mixing in the Thermocline: A Review. *Journal of Geophysical Research: Oceans*, 92(C5), pp. 5249-5286. https://doi.org/10.1029/JC092iC05p05249

24. Alford, M.H., 2003. Redistribution of Energy Available for Ocean Mixing by Long-Range Propagation of Internal Waves. *Nature*, 423, P. 159-162. doi:10.1038/nature01628

25. Forristall, G.Z., Larrabee, R.D. and Mercier, R.S., 1991. Combined Oceanographic Criteria for Deepwater Structures in the Gulf of Mexico. In: OTC, 1991. *The 23d Offshore Technology Conference*. Houston, USA. Paper OTC6541, pp. 377-390. https://doi.org/10.4043/6541-MS

26. Ivanov, V.P. and Pudov, V.D., 1977. [Structure of the Thermal Wake of Tess Typhoon in the Ocean and Estimation of Some Parameters of Energy Exchange under Storm Conditions]. In: V. N. Ivanov and N. I. Pavlov, 1977. [*Typhoon-75*]. Leningrad: Gidrometeoizdat. Vol. 1, pp. 66-82 (in Russian).

27. Pudov, V.D., Varfolomeev, A.A. and Fedorov, K.N., 1978. *Vertical Structure of a Typhoon Trace in the Upper Ocean. Oceanology*, 18*(*2), pp. 218-225 (in Russian).

28. Plekhanov, Ph.A. and Kovalev, D.P., 2016. The Complex Program of Processing and Analysis of Time-Series Data of Sea Level Based on the Original Algorithms. *Geoinformatika*, (1), pp. 44-53. Available at: http://geoinformatika.ru/wp-content/uploads/2020/06/Geo2016_1_44-53-1.pdf [Accessed: 21 January 2021] (in Russian).

29. Kunze, E., 1985. Near-Inertial Wave Propagation in Geostrophic Shear. *Journal of Physical Oceanography*, 15(5), pp. 544-565. https://doi.org/10.1175/1520-0485(1985)015<0544:NIWPIG>2.0.CO;2

30. Price, J.F., Sanford, T.B. and Forristall, G.Z., 1994. Forced Stage Response to a Moving Hurricane. *Journal of Physical Oceanography*, 24(2), pp. 233-260. https://doi.org/10.1175/1520-0485(1994)024<0233:FSRTAM>2.0.CO;2

31. Garrett, C., 2001. What is the ‘‘Near-Inertial’’ Band and Why is It Different from the Rest of the Internal Wave Spectrum? *Journal of Physical Oceanography*, 31(4), pp. 962-971. https://doi.org/10.1175/1520-0485(2001)031<0962:WITNIB>2.0.CO;2

32. Hou, H., Yu, F., Nan, F., Yang, B., Guan, S. and Zhang, Y., 2019. Observation of Near-Inertial Oscillations Induced by Energy Transformation during Typhoons. *Energies*, 12(1), 99. doi:10.3390/en12010099

33. Gill, A.E., 1984. On the Behavior of Internal Waves in the Wakes of Storms. *Journal of Physical Oceanography*, 14(7), pp. 1129-1151. https://doi.org/10.1175/1520-0485(1984)014<1129:OTBOIW>2.0.CO;2

34. Zervakis, V. and Levine, M.D., 1995. Near-Inertial Energy Propagation from the Mixed Layer: Theoretical Considerations. *Journal of Physical Oceanography*, 25(11), pp. 2872-2889. https://doi.org/10.1175/1520-0485(1995)025<2872:NIEPFT>2.0.CO;2

35. Kurkina, O.E., Talipova, T.G., Soomere, T., Kurkin, A.A. and Rybin, A.V., 2017. The Impact of Seasonal Changes in Stratification on the Dynamics of Internal Waves in the Sea of Okhotsk. *Estonian Journal of Earth Sciences*, 66(4), pp. 238-255. http://doi.org/10.3176/earth.2017.20

36. Nurser, A.J.G. and Bacon, S., 2014. The Rossby Radius in the Arctic Ocean. *Ocean Science*, 10(6), pp. 967-975. doi:10.5194/os-10-967-2014

37. Rayson, M.D., Ivey, G.N., Jones, N.L., Lowe, R.J., Wake, G.W. and McConochie, J.D., 2015. Near-inertial ocean response to tropical cyclone forcing on the Australian North-West Shelf. *Journal of Geophysical Research: Oceans*, 120(12), pp. 7722-7751. doi:10.1002/2015JC010868

38. Stepanov, D.V., 2017. Estimating the Baroclinic Rossby Radius of Deformation in the Sea of Okhotsk. *Russian Meteorology and Hydrology*, 42, pp. 601-606. https://doi.org/10.3103/S1068373917090072.

39. Byun, S.-S., Park, J.J., Chang, K.-I. and Schmitt, R.W., 2010. Observation of Near-Inertial Wave Reflections within the Thermostad Layer of an Anticyclonic Mesoscale Eddy. *Geophysical Research Letters*, 37(1), L01606. doi:10.1029/2009GL041601

40. Kawaguchi, Y., Wagawa, T. and Igeta, Y., 2020. Near-Inertial Internal Waves and Multiple-Inertial Oscillations Trapped by Negative Vorticity Anomaly in the Central Sea of Japan. *Progress in Oceanography*, 181, 102240. https://doi.org/10.1016/j.pocean.2019.102240

41. Kawaguchi, Y., Wagawa, T., Yabe, I., Ito, D., Senjyu, T., Itoh, S. and Igeta, Y., 2021. Mesoscale-Dependent Near-Inertial Internal Waves and Microscale Turbulence in the Tsushima Warm Current. *Journal of Oceanography*, 77(2), pp. 155-171. doi:10.1007/s10872-020-00583-1

42. Garrett, C.J.R. and Munk, W.H., 1972. Space-Time Scales of Internal Waves. *Geophysical Fluid Dynamics*, 3(3), pp. 225-264. https://doi.org/10.1080/03091927208236082

About the authors:

Peter D. Kovalev, Leading Research Associate, Institute of Marine Geology and Geophysics, Far Eastern Branch of Russian Academy of Sciences (1b Nauki Str., Yuzhno-Sahalinsk, 693022, Russian Federation), Dr. Sci. (Engineer.), **ORCID ID: 0000-0002-7509-4107**, **SCOPUS Author ID:16429135400**, **ResearcherID: V-8662-2018**, p.kovalev@imgg.ru

Vernon A. Squire, Professor, Department of Mathematics & Statistics, University of Otago (Dunedin 9054, New Zealand), **ORCID ID: 0000-0002-5570-3446**, **SCOPUS Author ID: 7004257488**, vernon.squire@otago.ac.nz

Dmitry P. Kovalev, Leading Research Associate, Institute of Marine Geology and Geophysics, Far Eastern Branch of Russian Academy of Sciences (1b Nauki Str., Yuzhno-Sahalinsk, 693022, Russian Federation), Dr. Sci. (Phys.-Math), **ORCID ID: 0000-0002-5184-2350**, **SCOPUS Author ID: 26032627700**, **ResearcherID: A-9300-2016**, d.kovalev@imgg.ru

Andrey I. Zaytsev, Acting Director, Special Design Bureau for Automation of Marine Research, Far Eastern Branch of the Russian Academy of Sciences (25, Alexey Gorky St.. Yuzhno-Sahalinsk, 693023, Russian Federation), Dr. Sci. (Phys.-Math), **ORCID ID: 0000-0002-138-3637**, **SCOPUS Author ID: 36866694500**, **ResearcherID: A-1772-2014**, a.zaytsev@mail.ru

Contributions of the co-authors:

Vernon A. Squire – methodology, conceptualization, investigation, formal analysis, writing original and submitted manuscripts, corresponding author

Peter D. Kovalev – methodology, data collection and curation, initial investigation, funding acquisition, preparatory drafting

Dmitry P. Kovalev – methodology, data collection and curation, initial investigation, funding acquisition, preparatory drafting

Andrey I. Zaytsev – methodology, data collection and curation, initial investigation, funding acquisition, preparatory drafting

All the authors have read and approved the final manuscript.
The authors declare that they have no conflict of interest.